

EXPERIMENTAL ANALYSIS ON AN ADDITIVELY MANUFACTURED ABS LIVING HINGE

Cassandra Gribbins*, Heidi M. Steinhauer, Ph. D*†

*Department of Mechanical Engineering, Embry-Riddle Aeronautical University, Daytona Beach, FL 32114

†Department of Engineering Fundamentals, Embry-Riddle Aeronautical University, Daytona Beach, FL 32114

Abstract

A study on the plastic behavior of an additively manufactured acrylonitrile butadiene styrene (ABS) living hinge was conducted using a MakerBot 2X. Initial research included numerical and analytical linear analyses on a typical living hinge design. This paper introduces the portion of the research that explores the application of traditional design practices to entry-level additive manufacturing machines. Tensile testing for material properties was conducted to refine the numerical model. Experimental rotational testing was conducted for data on the non-linear, plastic behavior experienced during application. Verification of the numerical model with experimental results will be used to guide future work on exploring alternate design geometries that leverage the advantages of additive manufacturing's design freedom for smoother stress distribution on the hinge.

Introduction

Inducing flexural capabilities within a single plastic piece is often executed through the utilization of a living hinge design. Bending is achieved by creating a relatively thin section of plastic between two larger, rigid regions. Incorporating living hinges in a design reduces part count which can result in lower overall costs and assembly time [1].

Initial research compared numerical and analytical analyses of a traditionally design living hinge against an alternate design. There was a large percent difference between stresses from the two solutions due to the analytical solution being conservative and the numerical solution overestimating the non-linear results. The initial research also indicated the hinges behaving in the plastic region under a small deformation of 10°. Comparing the calculated stresses with the yield strength to determine hinge behavior showed that all cases acted within the plastic region under the enforced deformation.

Further research suggestions to refine the results included testing for more applicable material properties for analysis and failure criteria of the living hinge. The initial research adjusted the yield strength of bulk ABS with respect to experimental investigations from Ahn et al. [2] and Rodriguez et al. [3] that demonstrated fused deposition modeled (FDM) ABS having 65 to 75% yield strength of injection molded ABS, resulting in a usable yield strength of 28.6 MPa. In Ahn et al.'s study [2] the common dogbone-shaped sample defined by the ASTM D638 standard was prone to break at the radii due to stress concentrations induced by gaps in the toolpath generation. The ASTM D3039 standard was then used for tensile testing [2]. Alternately, Lee and Huang [4]

conducted fatigue testing using the ASTM D638 standard and did not report any interference of results when a few samples fractured at the radii.

In Rodriguez et al.'s [3] research, the ASTM D3039 standard was also used to conduct tensile testing. They concluded a more significant reduction of 22 to 57% in strength relative to ABS monofilament [3]. This reduction is due in part by voids formed during the process. Default building parameters inherently resulted in voids within generated toolpath previews. Hossain et al. [5] demonstrated a visual feedback method of adjusting building parameters based on a magnified optical image of the printed part as modifications of parameters using the toolpath preview resulted in gaps that were not identified within the preview.

Toolpaths and other building parameters like build orientation affect the strength of the part inducing an anisotropic nature in FDM created parts. Properties can be considered isotropic within the x-y plane, while strength in the z-direction is measurably less due to the tendency to delaminate between layers [6].

Gibson et al. [6] investigated a traditional design of living hinge using a PolyJet 3D printing technology that utilizes photopolymer material [6]. Initial results indicated success but encourages further testing for heavy use. Stratasys, Ltd [7] reports manufacturing an FDM living hinge that lasts up to thousands of cycles. Build recommendations include printing living hinges in a vertical build orientation for the best hinge durability as shown in Figure 1. AM living hinges still have room for improvement as traditionally injection molded polypropylene living hinges that can last millions of cycles [8].

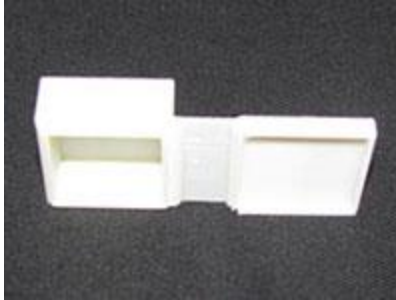


Figure 1 FDM living hinge printed in the vertical build orientation [7]

Experiments

Material Testing

Tensile testing for material properties was conducted to refine the material properties used in the CATIA V5 numerical model. Young's modulus influences how the stress is determined from the deformation/strain on the part. The yield strength sets the failure limit for designing a living hinge to act within the elastic region.

Tensile testing was conducted using the Tinius Olsen Model 290 Lo-Cap Universal Testing Machine with a 133,500 N load capacity. A Tinius Olsen S-400-2A extensometer was used to obtain strain data during tensile testing as shown in the testing setup in Figure 2. The strain rate applied was variable with an average of 20 mm/min.

Initial tensile testing was performed to determine proper design geometry between ASTM D3039 [9] and ASTM D638 Type I [10]. The specimen adhering to ASTM D3039 fractured within the grips while the ASTM D638 specimen fractured at the base of the radii similar to the results reported by Ahn et al. [2].

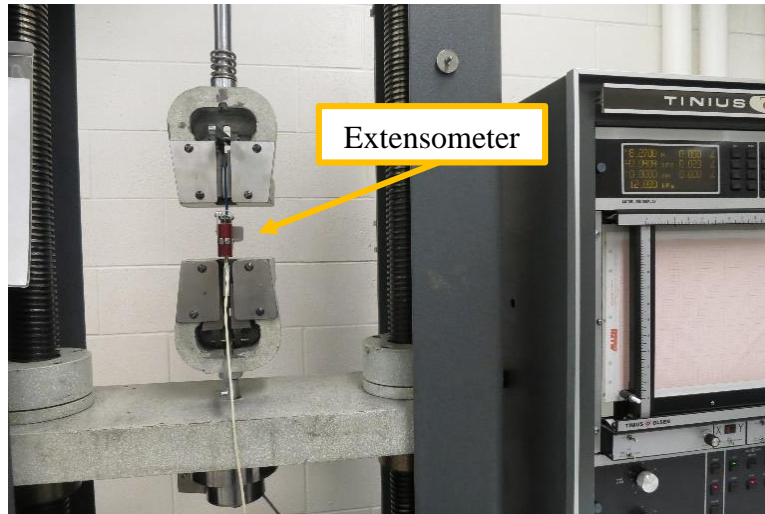


Figure 2 Tensile testing setup in the Tinius Olsen with extensometer attached

For the second iteration, 1/8” thick aluminum tabs were applied to the ends of the specimen for better grip and to prevent fracturing within the grips. Another tensile test resulted in the ASTM D3039 specimen fracturing at the location of the tabs. The ASTM D638 specimen again fractured at the base of the radii. Figure 3 shows the second iteration specimen failure.



Figure 3 Second iteration tensile testing specimen showing ASTM D638 at top fractured at the radii and ASTM D3039 fractured at the tab

The ASTM D638 design geometry was chosen for further testing as it did not fracture within the tab. The crazing displayed along the narrow length of the specimen was more evenly distributed for the ASTM D638 sample, as shown in Figure 4a. The crazing in the ASTM D3039 specimen was more concentrated toward the location of fracture as shown in Figure 4b.



Figure 4 Close-up image of crazing in a) ASTM D638 and b) ASTM D3039

Further refinement of the testing specimen included elongating the ends for more grip and decreasing the thickness to compensate for the additional thickness provided by the tabs. The testing area remained the same otherwise. Figure 5 displays the quarter base sketch used to generate the tensile specimen. The overall thickness of the part was 3.5 mm.



Figure 5 CATIA V5 base sketch of one quarter of the tensile specimen (units in mm)

The CATIA V5 part was exported to an (stereolithography) STL file with a sag size of 0.001 mm and imported into MakerBot Desktop to generate the toolpath data for printing. The specimen were all arranged to build in the vertical orientation as shown in Figure 6. The specimen were created in the vertical build orientation as the living hinges were also printed vertically. The same print orientation as the living hinge would provide material properties that represent the hinge structure.

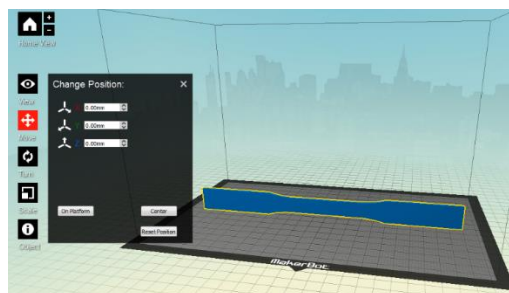


Figure 6 MakerBot Desktop Home View position of tensile specimen in vertical print orientation with coordinate system shown under the Change Position box (support structure not shown)

As a result of the vertical orientation, support material was generated to support the part underneath the curve. There is limited control over generation of toolpath direction under the main options so techniques on optimizing building parameters were not utilized. The standard print profile with default values from MakerBot Desktop were used although the infill was changed to 100% for a solid part. Toolpath preview was reviewed and discovered that MakerBot Desktop automatically generates a 45°/-45° alternating toolpath for the outer three layers on a part along the X-Y plane and switches to 0°/90° toolpath for the layers in between. Figure 7 illustrates a layer of the tensile specimen that combines the 45°/-45° toolpath for the outer layer of the narrow length of the part and the continuation of the 0°/90° for the left wide tab end. The standard setting also resulted in the presence of voids within the structure as indicated by the print preview.

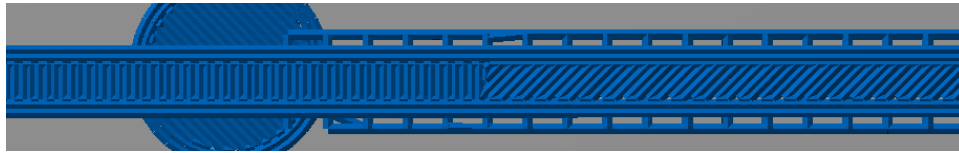


Figure 7 MakerBot Desktop top view of the print preview illustrating 0°/90° toolpath on the left and 45°/-45° for the outer layer of the narrow length on the right

The original cross-sectional area to be used in material property calculations was obtained by taking the average of the width and thickness measurements from the narrow section of the tensile specimen. The measurement locations are shown by the black markings in Figure 8 using Pittsburg 6” digital calipers with a resolution of 0.01mm.

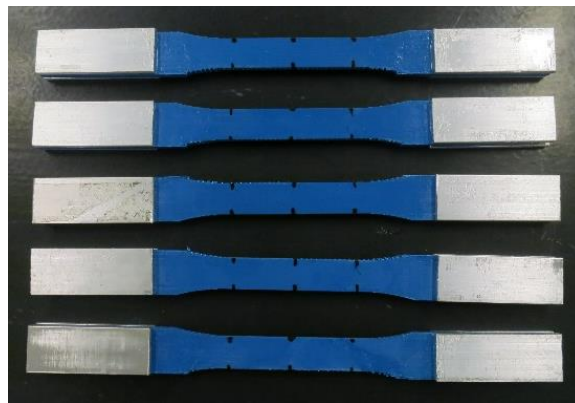


Figure 8 Third iteration tensile testing specimen

Application Testing

Experimental testing was planned to be conducted for data on the non-linear, plastic behavior experienced during application, but the micro-tensile machine to be used was unavailable. Fabricating of a living hinge was carried out to determine machine capabilities.

The model containing the traditional living hinge design, as shown in Figure 9, was created in CATIA V5. The minimum thickness of 0.3 mm for the hinge thickness would not be rendered by the MakerBot Desktop software in the print preview window when oriented in the vertical print

orientation. The hinge thickness was increased by 0.1 mm increments until the MakerBot Desktop software rendered the hinge section in the print preview.

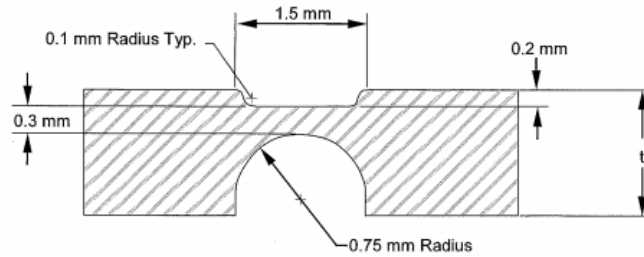


Figure 9 Traditional living hinge design [1]

The minimum hinge thickness that MakerBot Desktop would render was 0.6 mm, indicating geometry less than 0.6 mm cannot be printed. The hinge length was also adjusted to 3 mm as demonstrated by the living hinge experimentation by Goenka [11]. The lower recess of the hinge was modified from a semi-circle shape as illustrated in Figure 9 to a straight lower fiber with a 0.2 mm radius. The uniform hinge thickness was utilized to follow design suggestions by Stratasys, Ltd [7]. The final design for a printable living hinge on the MakerBot 2X is shown in Figure 10.

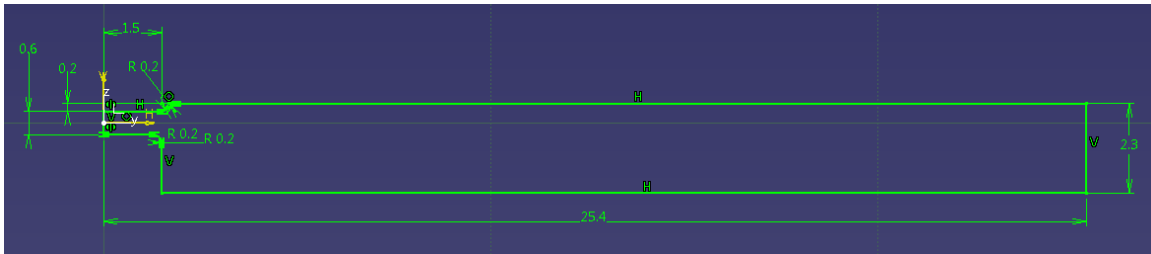


Figure 10 CATIA sketch of half a living hinge

The solid model in CATIA was characterized as a material with the Young's modulus and yield strength determined from tensile testing as shown in Figure 11. The remaining properties were obtained from CES EduPack 2013 [12]. Isotropic material was selected as the anisotropic option contained many necessary properties that were not available.

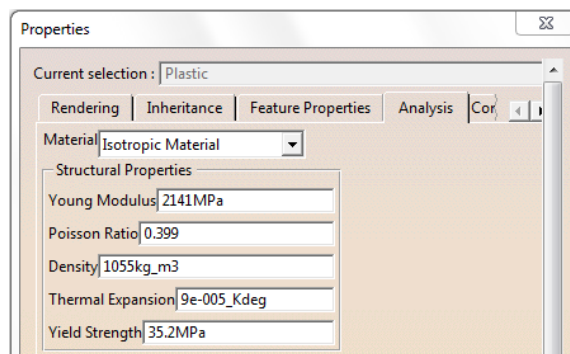


Figure 11 Material properties used in the FEA

CATIA V5's Generative Structural Analysis workbench was used to perform a finite element analysis (FEA) on the solid model. The left face was fully constrained and an enforced displacement was applied on the right end surface as shown in Figure 12. A vertical displacement of 4.5 mm was applied for a comparable 10° rotation. The enforced displacement was defined to use the axis system at the center of the hinge to encourage circular bending

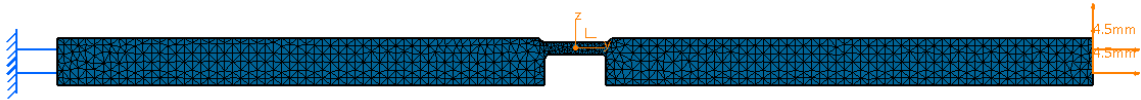


Figure 12 FEA case model

An overall part mesh of 0.4mm was generated by CATIA based on the part dimensions. A local mesh size around the hinge area was refined until the resultant maximum von Mises stress was within 3% of the previous 3 cases. Figure 13 displays the local mesh refinement of 0.16 mm about the hinge.

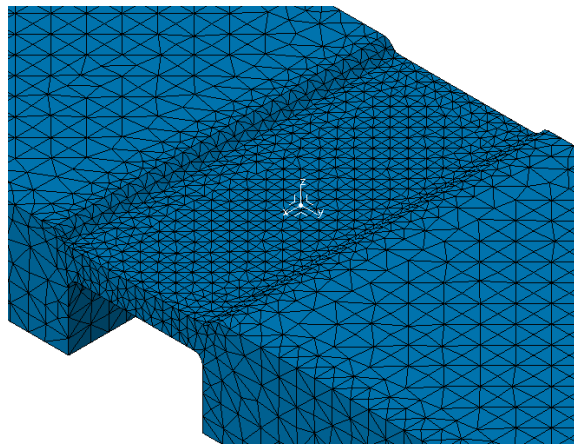


Figure 13 FEA local mesh refinement

Furthermore, five living hinge samples were printed and measured for comparison between the theoretical dimensions and the resulting print after shrinkage, which for ABS is generally about 2% [13]. All hinge specimen were printed in the vertical orientation as recommended by Stratasys, Ltd [7]. The print settings were set to the low/fast setting for MakerBot adjusting only the infill to 100%, the number of shells to 1, and reducing the layer height to the standard setting of 0.2 mm.

Results and Discussion

Material Testing Results

The fracture surface of the ASTM D3039 specimen from the second iteration was examined using a FEI Quanta 650 Scanning Electron Microscope (SEM) under the low vacuum setting. Voids similar to the one shown in Figure 14 were discovered. The depth and smooth walls of the void suggests that it was created during manufacturing and not a microvoid from part of the crazing.

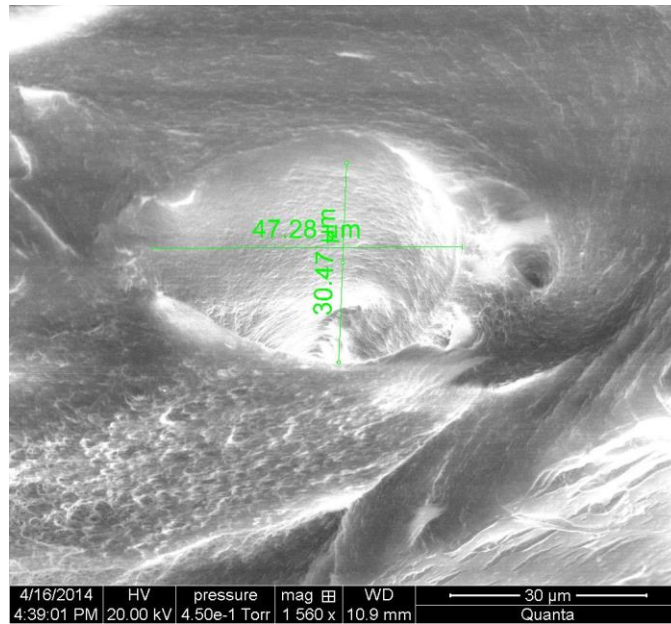


Figure 14 Scanning Electron Microscope (SEM) image of tensile testing specimen fracture surface illustrating void measurement of 47.28 μm by 30.47 μm

The measurements for the third iteration of tensile specimen are shown in Table 1. The results did not show any pattern on how the values differed at various areas across the narrow section. The thickness was considerably smaller than the theoretical and is attributed to the tendency for ABS to shrink approximately 2%.

Table 1 Tensile testing measurements for determination of usable cross-sectional area

Build Orientation	Specimen Number	Width (mm)							Thickness (mm)							Cross-sectional Area, A_0 (mm^2)	
		W1	W2	W3	W4	W5	Overall Average (mm)	SD	T1	T2	T3	T4	T5	Overall Average (mm)	SD		
Theoretical		13.00							3.50							45.50	
Vertical	I	13.02	12.97	12.96	12.99	12.98	12.98	0.0206	3.36	3.37	3.37	3.36	3.36	3.36	3.36	0.0049	43.68
	II	13.16	13.19	13.19	13.17	13.12	13.17	0.0258	3.47	3.49	3.51	3.52	3.52	3.50	0.0194	46.11	
	III	13.17	13.15	13.12	13.09	13.18	13.14	0.0331	3.37	3.37	3.36	3.36	3.36	3.36	0.0049	44.21	
	IV	13.02	13.06	13.04	12.98	13.00	13.02	0.0283	3.41	3.41	3.41	3.42	3.41	3.41	0.0040	44.42	
	V	13.08	13.07	13.08	13.06	13.07	13.07	0.0075	3.41	3.41	3.41	3.41	3.41	3.41	0.0000	44.58	
	Sectional Average	13.09	13.09	13.08	13.06	13.07	13.08		3.40	3.41	3.41	3.41	3.41	3.41		44.60	
SD	0.0728	0.0856	0.0861	0.0779	0.0831			0.0434	0.0490	0.0593	0.0654	0.0653					

From the third iteration, all five specimen fractured at the yield strength displaying brittle behavior. The failed specimen are shown in Figure 15. As shown, the fracture occurred at the base of the radii but still across an area similar to that measured across the narrow length. A lower strain rate may encourage more plastic behavior.

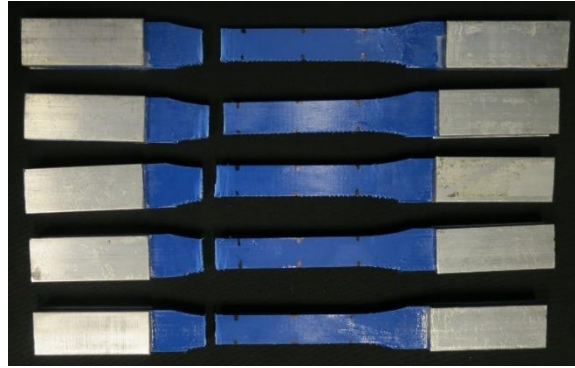


Figure 15 Tensile test specimen failure

The engineering stress vs strain curves from the third iteration are displayed in Figure 16. The curve displays the same characteristics as Rodriguez et al. [3] for a test specimen with fibers running perpendicular to the load direction. The fracture toughness of the material may have an influence on the brittle fracture of the specimen if the microvoid is greater than the allowable flaw size. The sample V3 appears to have experienced some slippage in the extensometer near the yield point of the curve, otherwise the results across the five specimen were consistent. The proportional limit of the curves were all around 15 MPa. The Young's modulus was calculated using points at the beginning and end of the modulus line as recommended by an instruction pamphlet from Tinius Olsen [14].

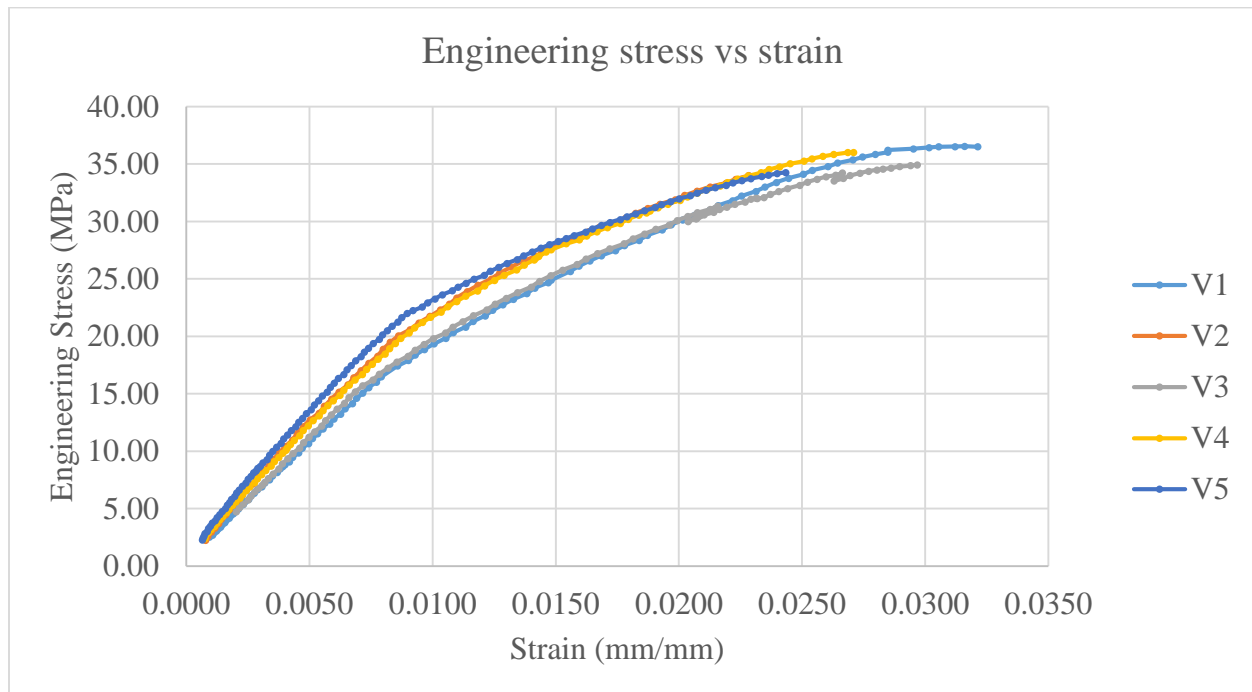


Figure 16 Engineering stress vs strain curves from the tensile specimen

The summary of determined material properties for each specimen and the overall average is shown in Table 2. The Young's modulus average of 2141 MPa and tensile strength average of 35.16 was used in the adjusted material properties for the CATIA V5 model.

CES EduPack 2013 [12] cites a range of values for each material property and for injection molded ABS the Young's modulus is stated as ranging from 2210 to 2620 MPa. The determined average for FDM ABS of 2141 MPa is 97% of the lower end of the injection molded material. The injection molded range for yield strength is 42 to 46 MPa resulting in the experimental yield strength of 35.2 being 84% of the lower end. The yield strength is a great improvement from previous material studies and can be attributed to the improvement of toolpath generating programs and overlapping fibers.

Table 2 Summary of material properties obtained from tensile testing

Specimen	Young's Modulus (MPa)	Yield Strength (MPa)	Yield Strain (mm/mm)
I	1983.59	36.56	0.0321
II	2219.82	34.01	0.0229
III	1985.16	34.93	0.0297
IV	2146.11	36.03	0.0271
V	2370.67	34.27	0.0243
Average	2141.07	35.16	0.0272
SD	147.01	0.99	0.0034

Application Testing Results

From the results of the tensile testing, the failure criteria is defined by stress beyond the yield strength of 35.2 MPa. The translational displacement diagram shown in Figure 17 verifies that the hinge deformed as expected about the center of the hinge.

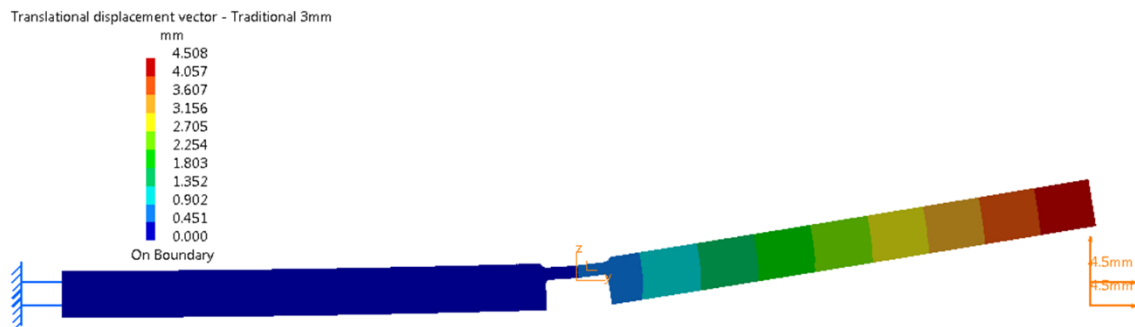


Figure 17 Translational displacement vector from CATIA V5 Generative Structural Analysis workbench

Figure 18 shows the von Mises stress distribution across the hinge with the yield stress of 35.2 MPa set as the maximum limit. High stress is experienced across the entire hinge with the highest stress experienced is 37.7 MPa under the lower portion of the hinge. This is above the yield stress under a 10° deformation. From the material testing, stress beyond the yield would result in fracture. This current design for a living hinge would not be practical for use with such a minimal operating range.

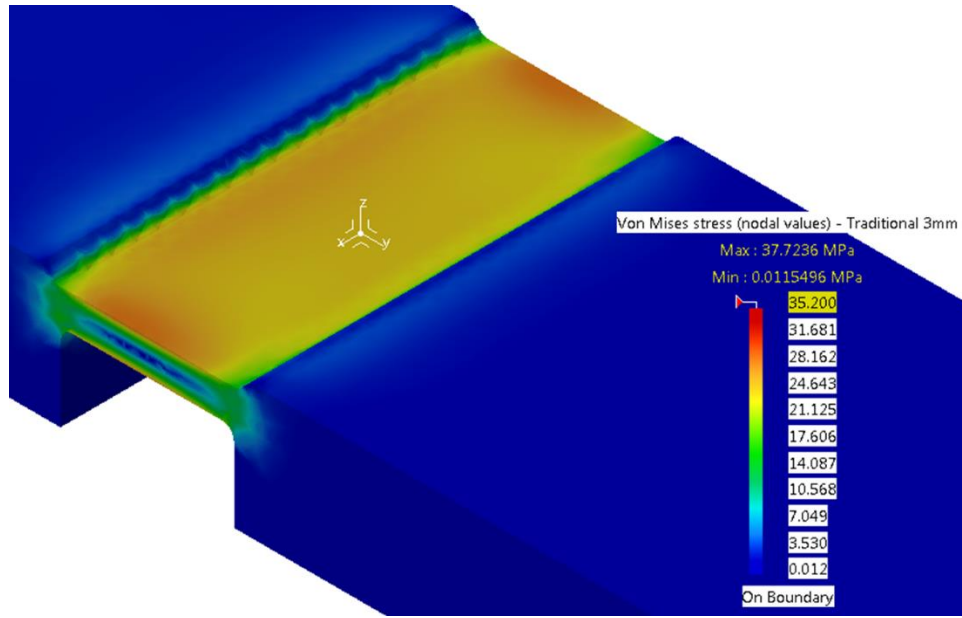


Figure 18 von Mises stress distribution from CATIA V5 Generative Structural Analysis workbench

Figure 19 displays the printed living hinges with the rearmost hinge placed in the vertical build orientation. It is interesting to note that due to the small design geometry, the lower portion of the hinge resulted in a curve close to the traditional design as shown in Figure 9.

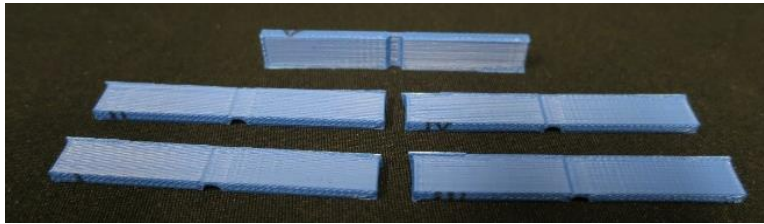


Figure 19 Manufactured living hinges with the rearmost hinge shown in the vertical build orientation

The results of the manufactured living hinge sample measurements are shown in Table 3. The length and width of the hinge dimensions were all lower than the theoretical while all of the measured thicknesses were all above the theoretical. The same pattern appeared in the overall dimensions with length and width both being lower than theoretical while thickness measured either at or slightly above the theoretical.

Table 3 Measurements for a set of traditional designed living hinges

		Hinge Dimensions			Overall Dimensions		
Specimen		Length (mm)	Width (mm)	Thickness (mm)	Length (mm)	Width (mm)	Thickness (mm)
Theoretical		3.00	7.40	0.60	50.80	7.40	2.30
Traditional	I	2.75	7.09	0.94	50.53	7.33	2.31
	II	2.71	7.11	0.93	50.46	7.27	2.30
	III	2.75	7.13	0.94	50.53	7.35	2.31
	IV	2.72	7.11	0.85	50.46	7.27	2.30
	V	2.77	7.12	0.92	50.48	7.25	2.30
	Average	2.74	7.11	0.92	50.49	7.29	2.30
	SD	0.0219	0.0133	0.0338	0.0319	0.0388	0.0049

When taking into account the expectation of ABS shrinking approximately 2%, the overall length and width averages are reasonable measurements while the length and width for the hinge portion are greater than the expected 2% shrinkage minimum. The effects of small hinge dimensions, as well as its location in the center of the part, may have contributed to a greater than expected shrinkage.

The theoretical value for hinge thickness, while shown to be large enough to manufacture in the print preview, was too small for the printer to create resulting in the apparent minimum thickness that can be printed as approximately 0.9 mm, although printers of similar capabilities can print to smaller values. The overall thickness resulted in nearly theoretical values.

Conclusion and Future Work

Tensile testing showed increased material property values from previously approximated tensile strength, 28.6 MPa to 35.2 MPa. The characteristics of the stress-strain curve displayed brittle behavior that can be attributed to the possibility of microvoids affecting the fracture toughness of the material. Future work into testing and determination of the fracture toughness property for FDM ABS is suggested. As advances in toolpath generation further minimize voids, determining the allowable flaw size is important when designing with respect to the critical stress of the structure.

As recommendations for future work, additional research for improving accuracy of small structures like living hinges using a MakerBot 2X would involve exploring the advanced options of MakerBot Desktop. Adjustment of the advanced options requires understanding of MakerBot terminology of the different parameters and how they affect the overall build.

Alternate designs for living hinges would be a study of interest for further research. The traditional design for a living hinge allows too high of a stress concentration in the small area as indicated by the FEA. Suggestions include elongating the hinge length or experimenting with completely new design geometries like zigzag or wave patterns.

References

- [1] P. A. Tres, *Designing Plastic Parts for Assembly*, 4th ed. Cincinnati: Hanser-Gardner, 2000.

- [2] S.-H. Ahn, M. Montero, D. Odell, S. Roundy, and P. K. Wright, “Anisotropic material properties of fused deposition modeling ABS,” *Rapid Prototyp. J.*, vol. 8, no. 4, pp. 248–257, 2002.
- [3] J. F. Rodríguez, J. P. Thomas, and J. E. Renaud, “Mechanical behavior of acrylonitrile butadiene styrene (ABS) fused deposition materials. Experimental investigation,” *Rapid Prototyp. J.*, vol. 7, no. 3, pp. 148–158, Aug. 2001.
- [4] J. Lee and A. Huang, “Fatigue analysis of FDM materials,” *Rapid Prototyp. J.*, vol. 19, no. 4, pp. 291–299, 2013.
- [5] M. S. Hossain, J. Ramos, D. Espalin, M. Perez, and R. Wicker, “Improving Tensile Mechanical Properties of FDM-Manufactured Specimens via Modifying Build Parameters,” in *International Solid Freeform Fabrication Symposium An Additive Manufacturing Conference*, Austin, Texas, 2013, vol. 2013, pp. 380–392.
- [6] I. Gibson, G. Goenka, R. Narasimhan, and N. Bhat, “Design Rules for Additive Manufacture,” in *International Solid Freeform Fabrication Symposium An Additive Manufacturing Conference*, Austin, Texas, 2010, vol. 2010, pp. 705–716.
- [7] Stratasys, Ltd., “Functional Prototyping - Living Hinges.” 2013.
- [8] J. M. Hoffman, “Care and feeding of living hinges,” *Machine Design*, vol. 76, no. 16, pp. 64, 66, 19-Aug-2004.
- [9] ASTM International., *Standard test method for tensile properties of polymer matrix composite materials*. West Conshohocken, Pa.: ASTM International, 2010.
- [10] A. S. D. 1. on M. P. ASTM Committee D-20 on Plastics., *Standard test method for tensile properties of plastics*. Philadelphia, Pa.: ASTM International, 2010.
- [11] G. Goenka, “Modeling and investigation of elastomeric properties in materials for additive manufacturing of mechanistic parts,” National University of Singapore, Singapore, 2011.
- [12] B., France, Anna Kaziunas., Shergill, Jay., Pettis, *Getting started with MakerBot*. Sebastopol, Calif.: O’Reilly, 2013.
- [13] “Interpretation of Stress-Strain Curves and Mechanical Properties of Materials.” Tinius Olsen Testing Machine Co., Inc.
- [14] CES EduPack 2013, “ABS (injection molding, platable).” Granta Design Limited, 2013.